Proceedings of the
International Conference on Mechanical Engineering 2005
(ICME2005) 28- 30 December 2005, Dhaka, Bangladesh

ICME05-TH-11

STUDY ON FORCED CONVECTION HEAT TRANSFER IN TRIANGULAR, TRAPEZOIDAL, SAW TOOTH FORWARD AND SAW TOOTH BACKWARD TYPES RIBBED WALL

Khan Rezaul Karim, M Morad Hossain Mollah, M A T Ali, M A R Akhanda and M A R Sarkar

Department of Mechanical Engineering, Bangladesh University of Engineering and Technology, Dhaka, Bangladesh.

ABSTRACT

The flow characteristics obtained in forced convection heat transfer with asymmetric heating has been carried out for turbulent flow through the developed region of a square duct. The duct is made of heat resisting materials, whose bottom surfaces for both the ducts are made of 12 mm thick aluminium sheets. The bottom surface of the rough duct is the rib-rough wall having roughened with triangular, trapezoidal and saw tooth (forwards and backward ribs). It is heated by passing electric current and uniform heating is controlled using a digital temperature controller and a variac. The experiments have been conducted for different Reynolds number varies from 5.0×10^4 to 5.6×10^4. It is found in the result that the Nusselt number increases by 0.850, 2.152, 1.280 and 18.779 percent in saw tooth forward ribbed wall over triangular, trapezoidal , saw tooth backward (p/e=6, Re=5.0×10^4) and non-ribbed wall with an increase of Reynolds number up to 12 percent . An empirical equation has been developed which correlates all data generated in testing and finally the result has been compared with other relations available in the literature.

Keywords: Saw Tooth backward and forward, Non- Ribbed wall, Friction Factor.

1. INTRODUCTION

Forced convection heat transfer in engineering application commonly encountered in engineering practice occur in a straight non-circular duct like; compact heat exchangers, cryogenic coolant systems, nuclear reactors, cooling tower, air conditioning systems, etc. Hirota [1-2], Han[3-4], Fijita[5-6] and Sparrow[7] have investigated heat transfer augmentation for fully developed turbulent flow with rib-roughened non-circular ducts. Melling [8] has conducted experimental studies with turbulent flow through non-circular smooth ducts in the developed region. It is found in the result that the rough side of a ribbed duct enhances heat transfer up to 2.4 times over the smooth side. It is also seen that rough ducts have flatter velocity profiles than the smooth duct and those flatter velocity profiles are responsible for producing higher heat transfer.

In this field most of the works, before sixty decade of this century, have been carried out with circular ducts. The vast majority of forced convection heat transfer work has involved the use of different fluids in heated circular duct either at constant temperature or at constant heat flux. James[9] have investigated the heat transfer characteristics in developed region with asymmetric heating of a non-circular duct and developed a correlation for the evaluation of Nusselt number. Hong[10], Monohar[11], Ulrichson[12] and Hwang[13] carried out experimental study on heat transfer phenomenon of laminar flow in the entrance region of circular tubes. It is seen in the literature survey that Sparrow is only the investigator who has conducted an investigation with laminar forced convection heat transfer in entrance region of non-circular ducts. So far as it is known, none have conducted experiments for turbulent forced convection heat transfer in entrance region of a non-circular duct. For this reason, researchers of present study are interested to investigate the heat transfer characteristics for turbulent flow through the developed region of ribbed and non-ribbed square duct.

2. EXPERIMENTAL SETUP

Figure 1 shows a schematic diagram of the experimental apparatus. Air at room temperature and standard pressure is introduced into the square duct after flowing through a contraction. The cross-sectional dimension of the duct is 50mm×50mm and its hydraulic diameter (D_h) is 50mm. It is ascertained that the fully developed velocity profiles have been attained about $50D_h$ (2500 mm) downstream from the entrance of the developing duct. The cross-sectional view of the duct is shown in Fig.2. The over all length of the duct is 5755mm, which is divided into three parts. They are the hydrodynamic developing duct of length 3000mm, the hydrodynamically developed duct of length 1830mm and the rear duct of length 925mm. The test duct is made of

insulating materials. Bakelite sheet of 16mm thick is used to make its side walls and supporting wall. The top wall is made of 12.5mm thick clear perspex sheet and is fastened with the side walls by means of Allen bolts.

A flexible duct (damper) is made of canvas and placed at the outlet of the rear duct. A diffuser of length 920mm made of 16-gauge mild steel sheet is introduced between the outlet of the flexible duct and the inlet of the fan motor having 2.75 hp and 2900 rpm. A silencer is introduced at the outlet of the fan motor to minimize creating sound and vibration. A butter-fly is set-up at the other end of the silencer to control flow rate of air for measuring the required Reynolds number. At the end of the butter fly, a 90^o-bent duct is used to exhaust air to vertically upward. All elements of the experimental set-up are mounted on stands with proper levelling, at a convenient height of about 1020mm from the base and different sections have been assembled to one another by means of flanges and nuts-bolts.

The bottom surface of the aluminium wall of the test duct heats uniformly with electricity, supplying electric power to the heater, The heater has been designed and constructed by wounding Nichrome flat wire around a mica sheet shown in Fig.3. The uniform heating is controlled using a digital temperature controller and a varaic. Six pressure taps are the length of the test duct to measure the static pressures Eleven thermocouples are distributed at eleven different positions along the length of 1530 mm, the bottom wall bisector to measure the temperatures at the outer surface of the aluminium wall. Thus the average temperature at the outer wall is calculated and the mean temperature at the inner surface of the aluminium wall is evaluated using the corrected equation.

Calibration of Manometers

One vertical manometer, one multi-inclined manometer, one micro-manometer, one auto ranging micro DMM are used to measure the air velocities at inlet and outlet cross sections of the test duct. Before using these manometers they are calibrated with a standard manometers in different ways to have the more accurate data.

In the first calibration measurements techniques are h (mm) of water vs. V (volt) 3% range. Initial manometer reading, h_i = 35 mm inclined manometer tube angle = 15 degree, specific gravity of manometric fluid = 0.79, initial voltmeter reading V_i = 0.014 volt, Range = 3%, Equation, h (mm) = 23.133 x – 0.4684. In the second calibration measurements techniques are h (mm) of water vs. v (volt) 1% range. Initial manometer reading h_i = 85 mm, initial manometer tube angle = 15 degree, specific gravity of manometric fluid = 0.79, initial voltmeter reading V_i = 0.025 volt, Range = 1%, Equation, h (mm) = 8.8491 x – 0.454.

In the third calibration measurements are ΔP vs. V (volt) 10% ΔP scale.

Initial manometer reading h_i = 29 mm, initial manometer tube angle = 30 degree, specific gravity of manometric fluid = 0.79. Initial voltmeter reading = 0.002 volt. Initial digital voltmeter reading = 0.00 mm of water. Equation, h (mm) = 40.082 x – 0.3216.

In the fourth calibration measurements technique are velocity vs. Voltage, 10% ΔP scale range.

Initial manometer reading h_i = 23 mm, initial manometer tube angle = 30 degree, specific gravity of manometric fluid = 0.79. Initial voltmeter reading = 0.0016 volt. Initial digital voltmeter reading = 0.1 m/sec. Equation, h (mm) = 37.577 x – 0.7614.

In the fifth calibration measurements technique are V (volt) vs. h (mm), Range 10%.

Initial manometer reading h_i = 29 mm, initial manometer tube angle = 15 degree, initial voltmeter reading V_i = 0.000 volt.Range = 10%, Equation h (mm) = 76.536 x – 0.9435. A pitot-static tube is installed at the entrance section (Hydro-dynamically entry region) to read the reference velocity easily.

3. WORKING PROCEDURES OF THE EXPERIMENT

At the beginning of every set of experiment, a specified target temperature is fixed to the temperature controller. The voltage and current supplied to the heater are recorded from a digital voltmeter and a digital ammeter and thus heat energy generated to the heater is calculated. Eleven thermocouples are positioned to the bottom surface of the aluminium wall to measure its temperatures. The distributions of thermocouples are at a distance of 163mm, along the bisector of the bottom surface and a digital thermocouple thermometer with a selector switch is used to record the temperatures at their respective positions. The mean temperature of the bottom surface is calculated by averaging the recorded temperatures and the mean temperature of its inner surface is evaluated using corrected equation.

The temperatures and velocities of the heated air flowing in the test duct are measured for 494 1n Y-Y axis and 507 in Z-Z axis specified points across its inlet and outlet. From the recorded data the average temperature and average velocity at inlet and outlet are calculated for every set of experiment. Thus, the mean temperature and mean velocity of flow are evaluated by averaging those average temperatures and average velocities. For each set of experiment, static pressures at wall are measured from six pressure-taps. The taps are mounted at a distance of 300mm in the range between X/D=3 to X/D=33 and at the same level of 25 mm below its top side. From the pressure difference along the length of the test duct the corresponding friction factors are evaluated. To have a clear understanding on the flow characteristics across the duct cross-section at X/D = 3, a plenty of data are recorded at seven different level like; Y/B = -0.9, -0.8, -0.7, -0.6, -0.4, -0.2 and 0.0.

4. RESULTS AND DISCUSSION

(i) Average temperature difference between outlet and inlet of the test duct

Figure 7 shows the effect of Reynolds number on the temperature difference between outlet and inlet of the test duct. The temperature decreases gradually from 3.56 ^{o}C to 2.925 ^{o}C with an increase of the Reynolds number in the range between 5.00×10^4 to 5.6×10^4 .It gives the total amount of decreasing about 17.84 percent. The reason of decreasing is that due to higher Reynolds

number, the mean velocity of air increases and instantaneously every particle of air have a less amount of sensible heat from the bottom heated aluminium surface than the flow having lower velocity. So average temperature of air at the exit of the test duct is lower for higher Reynolds number rather than the lower one.

(ii) Effect of Reynolds number on heat energy absorbed by air flowing in the duct

Figure 4 is an example of the effect of Reynolds number on heat energy absorbed by air flowing through the duct. It is seen that the enthalpy of the air flowing in the duct increases with an increase of Reynolds number. This is because, due to higher Reynolds number, the mass flux is increasing more than the lower Reynolds number at any interval of time. Actually, the heat absorbed to the air by the process of convection is directly proportion to the specific heat of air, cross-sectional area of the duct, mass flux and the temperature difference between the outlet and inlet of the test duct. In this context, cross sectional area is constant, for a mean temperature specific heat of air is considered to be constant, the temperature difference is decreasing and the mass flux is increasing. In the analysis it is observed that the amount of increasing mass flux is more than the amount of decreasing the temperature difference. That is why, the amount of enthalpy increasing by the air flowing in the duct gradually with increasing Reynolds number and for the tests it increases by 0.850, 2.107, 1.264 and 15.864 percent in saw tooth forward ribbed wall over triangular, trapezoidal , saw tooth backward (p/e=6, Re=5.0 × 10^4) and non-ribbed wall with an increase of Reynolds number up to 12 percent .

(iii) Effect of Reynolds number on Nusselt number

Figure 5 shows the effect of Reynolds number of Nusselt number. From the analysis, it is seen that the convection heat energy absorbed by the air flowing in the duct is increasing as increasing the heated surface area, and the temperature difference between the inner surface temperature of the aluminium wall and the mean temperature of flow. The inner surface temperature of the aluminium wall is almost same in all tests but the mean temperature of air decreases with an increase of Reynolds number. This is because, higher Reynolds number decrease the average temperature of flow at inlet and outlet of the test duct. Thus, the heat transfer coefficient increases with an increase of heat addition to the air flowing in the duct. The higher value of average heat transfer coefficient yields the higher value of average Nusselt number. In the tests it is observed that both the average heat transfer coefficient and the average Nusselt number are increased by 0.850, 2.152, 1.280 and 18.779 percent in saw tooth forward ribbed wall over triangular, trapezoidal , saw tooth backward (p/e=6, Re=5.0×10^4) and non-ribbed wall with an increase of Reynolds number up to 12 percent**.**

(iv) Effect of Reynolds number on Stanton number

Figure 6 shows the effect of Reynolds number on Stanton number. In the analysis, it is seen that the Stanton number decreases with an increase of Reynolds number. Stanton number is directly proportion to the heat transfer coefficient and inversely proportion to the density, specific heat, and mean velocity of flow for a particular mean temperature of air. In the experiments, it is observed that mean velocity of flow increases more than the heat transfer coefficient for the increase the Reynolds number. For this reason, Stanton number decreases with an increase of Reynolds number and in the tests it is seen tha Stanton number decreases by 4.963, 5.229, 5.313, 5.279 and 3.379 percent in triangular, sawtooth forward, trapezoidal and saw tooth backward (p/e=6, Re=5.0×10^4) and non-ribbed wall with an increase of Reynolds number up to 12 percent.

(v) Development of Correlations

Figures 10-11 shows the curve fitting to the data obtained from the exeriments of the ducts having ribbed and smooth walls.The curve fittings have developed two correlations, which are used for the determination of forced convection heat transfer in the similar types ducts with ribbed wall and smooth wall as given in the following equations

$$\frac{Nu\,(2+1.6\,e^{-As})}{\frac{Pr^{0.4}}{e^{0.0134\,Pr}}\mu_r^{-0.8}} = 0.172\,Re^{(0.0016\,Pr+0.75)}$$

for smooth wall (1)

$$\frac{Nu\,(2.05+1.62e^{-As})}{\frac{Pr^{0.4}}{e^{0.0134\,Pr}}\mu_r^{-0.8}(p/e)^{-0.13}} = 0.175\,Re^{(0.0016\,Pr+0.75)}$$

for ribbed wall (2)

5. CONCLUSIONS

(i) In this research, it is seen that the average air temperature differences between the outlet and inlet of the test duct decreases by 17.84 percent.

(ii) The stanton number decreases by 4.963, 5.229, 5.313, 5.279 and 3.379 percent in triangular, sawtooth forward, trapezoidal and saw tooth backward (p/e=6, Re=5.0 × 10^4) and non-ribbed wall with an increase of Reynolds number up to 12 percent. .

(ii) It is seen that for an increase of Reynolds number up to 12 percent; mass flux, enthalpy increases to the air and average Nusselt number are increased by 12.284, 7.831, and 6.376 percent in saw tooth forward , 12.248, 7.214 and 6.320 percent in saw tooth backward, 12.248, 7.794 and 6.674 percent in triangular 12.248, 7.736 and 6.282 percent trapezoidal ribbed wall (p/e=6) and 12.248, 8.797, and 8.452 percent non- ribbed wall respectively.

(iii) The comparisons between the Nusselt number against Reynolds number are made among the experimental result.

(iv) It is seen that for an increase of Reynolds number up to 12 percent with decreases the friction factors

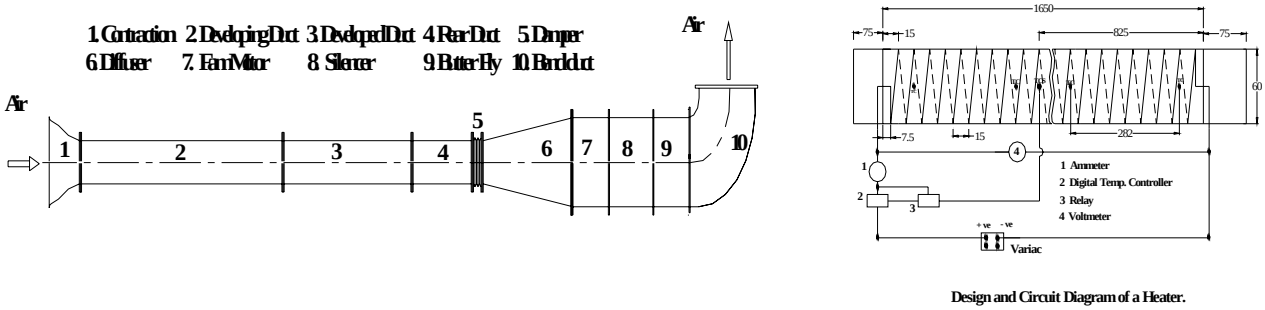

Fig 1. The Schematic diagram of the experimental apparatus

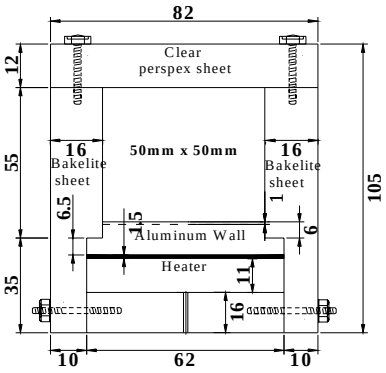

Fig 2. The End view of the test duct

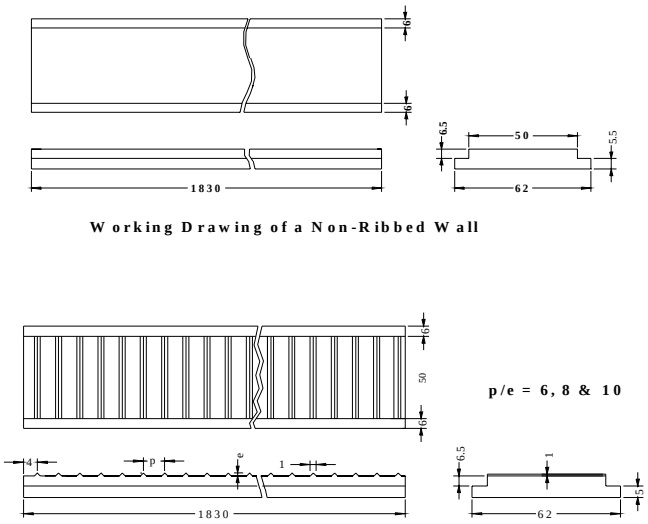

Fig 3. Working Drawing of a Ribbed Wall

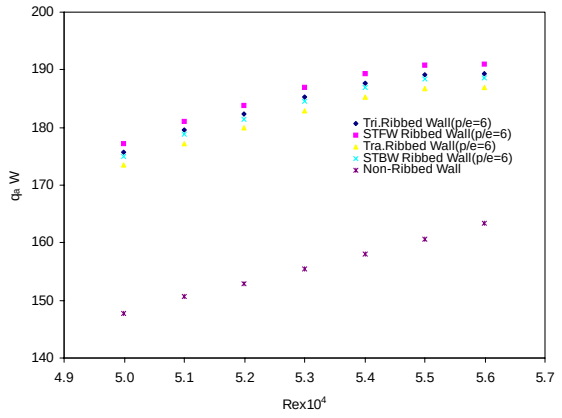

Fig 4. Effect of Reynolds number on Heat absorbed of Various types of Ribbed Wall

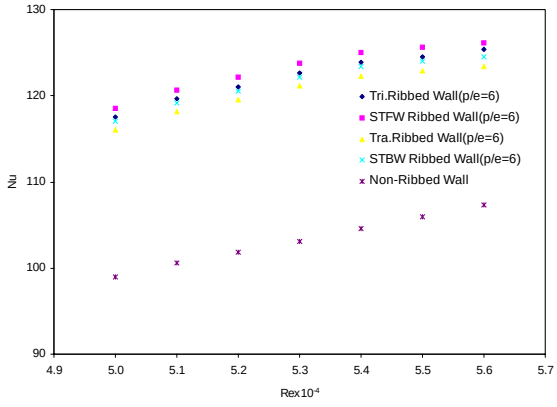

Fig 5. Effect of Nusselt number on Reynolds number on various types of Ribbed Wall

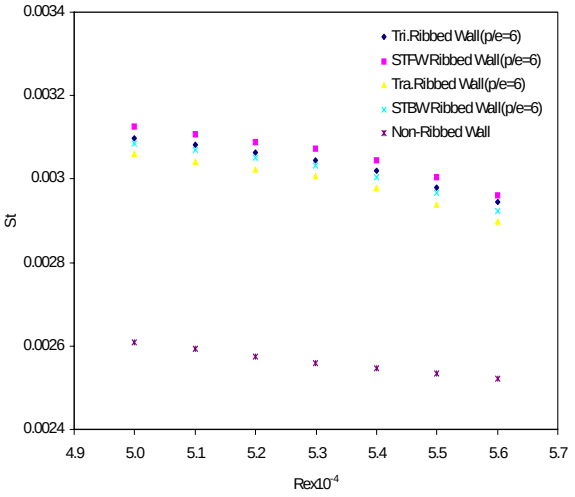

Fig 6. Effect of Stanton number on Reynolds number of various types of Ribbed Wall

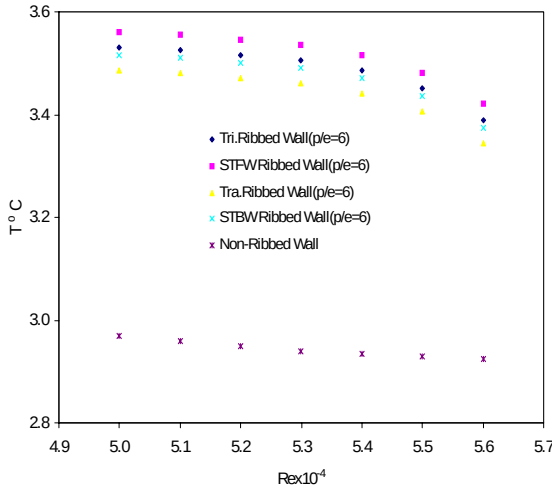

Fig 7. Effect of Reynolds number on Temperature Difference of various types of Ribbed Wall

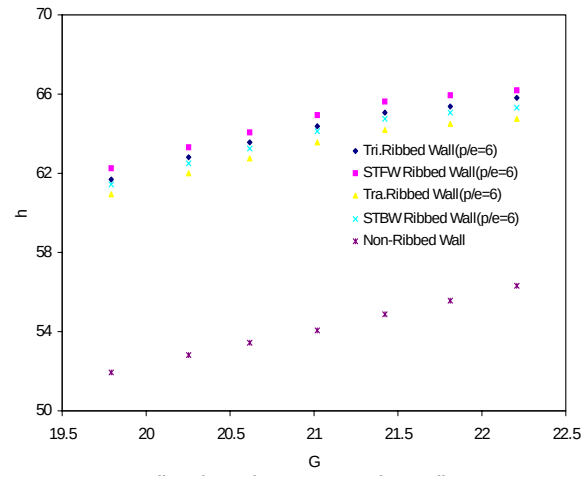

Fig 8. Effect of Mass flux on heat Transfer co-efficient of various types of Ribbed Wall

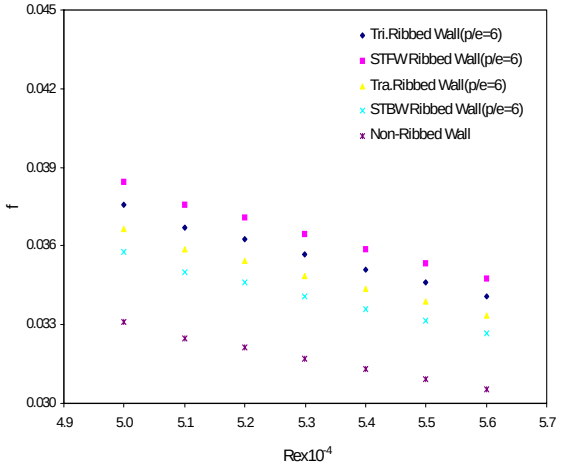

Fig 9. Effect of Friction Factor on Reynolds number of various types of Ribbed Wall

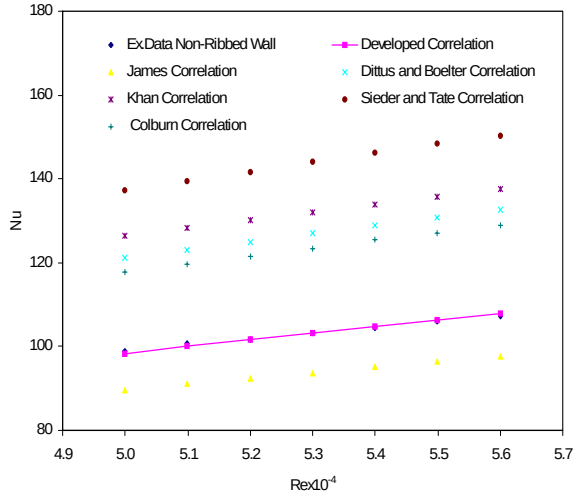

Fig 10. Developed Correlation for Non-Ribbed Ducts in Hydrodynamically Developed region

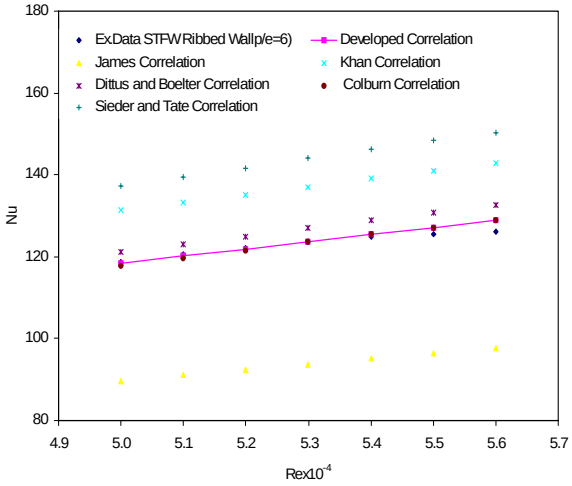

Fig 11. Developed Correlation for Ribbed Ducts in Hydrodynamic Developed region

9.290, 9.553, 9.013, 8.723 and 7.758 in triangular,saw tooth forward,trapezoidal,saw tooth backwardand non-ribbed wall at the rib pitch to height ratio of p/e=6.

6. ACKNOWLEDGEMENT

The authors express their thanks to all the staffs of different workshops and laboratories for their co-operation in producing the experimental set up. They also thank Professor Md. Abul Bashar, Director General, Directorate of Technical Education for allowing Md. Morad Hossain Mollah to pursue his Ph.D Engineering work.

7. REFERENCES

1. Hirota. M., Fujita. H., and Yokosawa. H.,1994, "Experimental Study on Convective Heat Transfer for Turbulent Flow in a Square Duct With a Ribbed Rough Wall (Characteristics of Mean Temperature Field)." Journal of Heat Transfer, Vol.116, pp. 332-340.
2. Hirota. M., Fujita. H., and Yokosawa,1980, "Forced Convective Heat Transfer in a Turbulent Flow through a Square Duct", Nagoya University, Vol. 40, No.2–Research report.
3. Han. J. C., and Park. J. S., 1988, "Developing Heat Transfer in Rectangular Channels with Rib-Turbulators." International Journal of Heat and Mass Transfer, Vol.31, pp.183-195.
4. Han. J. C., Park. J. S., and Lie. C. K., "Heat Transfer Enhancement in Channels with Turbulent Promoters." ASME, Journal of Engineering for Gas Turbines and Power, Vol.107,
5. Fujita. H., Hirota. M., and Yokosawa. H., 1990, "Experiment of Turbulent Flow in a Square Duct with a Roughened Wall." Memoirs of Faculty of Engineering, Nagoya University, Vol.41, No.2, pp.280-291.
6. Fujita. H., Hirota. M., and Yokosawa. H., 1989, "Forced Convection Heat Transfer in a Turbulent Flow Through a Square Duct." Mem. Faculty of Engineering, Nagoya University, Vol.40, No.2, pp.327-336.
7. Sparrow. E. M., 1985, "Analysis of Laminar Forced Convection Heat Transfer in Entrance Region of Flat Rectangular Ducts," NACA Tech Notes, TN 3331, 1955. pp.628-635.
8. Melling. A., and Whitelaw. J. H., 1976, "Turbulent Flow in a Rectangular Duct", J. Fluid Mech., Vol. 78, part 2, pp. 289-315.
9. James, D. D, 1967, "Forced convection Heat Transfer in ducts of Non-circular section." Ph.D Thesis, Imperial College, University of London, U.K.
10. Hong. S. W., and A. E. Bergles, 1976, "Laminar Flow Heat Transfer in the Entrance Region of Semi-Circular Tubes with Uniform Heat Flux." International Journal of Heat and Mass Transfer, Vol.19, pp123-124.
11. Monohar. R., 1969,"Analysis of Laminar Flow Heat Transfer in the Entrance Region of Circular Tubes," International Journal of Heat and Mass Transfer, Vol.12, pp.15-22.
12. Ulrichson. D. L., and R. A. Schmitz., 1965,"Laminar Flow Heat Transfer in the Entrance Region of Circular Tubes," International Journal of Heat and Mass Transfer, Vol.8, pp253-258.
13. Hwang. C. L., and Fan L. T., 1964, "Finite Difference Analysis of Forced Convection Heat Transfer in Entrance Region of a Flat Rectangular Duct." Appl. Sci. Res., Sec. A Vol.13, pp.401-422.
14. Akhanda. M. A. R., 1985, "Enhancement Heat Transfer in Forced Convective Boiling," Ph.D Thesis, University of Manchester Institute of Science and Technology, U.K.

8. NOMENCLATURE

Symbol	Meaning	Unit
A_c	Cross sectional area of the test duct	(m^2)
A_s	Surface area of the aluminium wall	(m^2)
B	Half of the side of test duct, D/2	(m)
D_h	Equivalent diameter of the duct	(m)
C_p	Specific heat of air	(J/kg^{o}C)
G	Mass flux of air flowing in the duct	(kg/m^2s)
Nu	Nusselt number	(-)
μ_b	Dynamic viscosity at mean temperature of air.	(Kg/m-s)
μ_w	Dynamic viscosity of air	(kg/m-s)
μ_r	μ_b / μ_w Viscosity ratio.	(-)
ρ	Density of air.	(kg/m^3)
q_g	Heat energy supplied to the heater	(W)
q_{cod}	Heat conducted through aluminium wall	(W)
q_a	Heat energy absorbed by air.	(W)
$q_{conv.}$	Heat energy convected to air	(W)
Pr	Prandtl number	(-)
Re	Reynolds number	(-)
St	Stanton number	(-)
T_{mi}	Average temperature at the inlet.	(^{o}C)
T_{mo}	Ave. temperature at outlet	(^{o}C)
T_m	Mean temperature of air in duct.	(^{o}C)
T_{wo}	Ave outer surface temp.of Al wall.	(^{o}C)
T_{wi}	Ave inner surface temp.of Al wall	(^{o}C)
T_c	Temp. at centre line of the duct	(^{o}C)
ΔT	($T_{mo} - T_{mi}$) Temp. difference bet^n outlet and inlet of the duct	(^{o}C)
u_{mi}	Average velocity at the inlet of the test duct.	(m/s)